

Hydrogen-related defects in ZnO studied by infrared absorption spectroscopy

E. V. Lavrov,* J. Weber, and F. Börrnert
Technical University of Dresden, 01062 Dresden, Germany

Chris G. Van de Walle
Palo Alto Research Center, 3333 Coyote Hill Road, Palo Alto, California 94304

R. Helbig
Institute for Applied Physics, University of Erlangen, Germany
 (Received 18 May 2002; published 3 October 2002)

Two hydrogen-related defects in ZnO are identified by a combination of local vibrational mode spectroscopy and first-principles theory. The H-I center consists of one hydrogen atom at the bond-center site oriented along the c axis of the crystal. The H-II center contains two inequivalent hydrogen atoms primarily bound to oxygen atoms. The polarized absorption data allow us to identify H-II as a zinc vacancy having two hydrogen atoms.

DOI: 10.1103/PhysRevB.66.165205

PACS number(s): 61.72.Ji, 61.72.Bb, 71.55.Gs, 78.30.Fs

I. INTRODUCTION

Due to recent progress in crystal growth¹ and unique piezoelectric, optical, and electrical properties, ZnO is considered at the moment as a serious alternative to GaN for use in optoelectronic devices.² ZnO nearly always exhibits n -type conductivity. The nature of this conductivity has been discussed for years and is normally attributed to native defects, such as the Zn-on-O antisite (Zn_O), the Zn interstitial (Zn_i), and the O vacancy (V_O).³ However, a new and unexpected cause for the n -type conductivity of ZnO has recently been proposed, first-principles investigations based on density-functional theory suggest that hydrogen in ZnO, unlike other semiconductors, occurs exclusively in the positive charge state, i.e., it always acts as a donor.⁴ Bond-centered (BC) and antibonding (AB) configurations were found to be close in energy for isolated interstitial H^+ . Recent muon spin rotation⁵ and (EPR) (Ref. 6) studies indeed confirmed the presence of hydrogen-related shallow donors. However, the molecular structure of these defects remains unknown.

Hydrogen is frequently present in the crystal-growth environment, and it is very difficult to avoid its incorporation into the crystal during the process of crystal growth. Thus, understanding of hydrogen properties in ZnO is necessary not only from an academic point of view but also for semiconductor applications. Infrared absorption is an excellent tool to perform this task. Knowledge about local vibrational modes (LVM's) gives detailed insight into the physical properties of light impurities embedded in ZnO. The frequencies of the LVM's reveal directly the chemical binding of hydrogen with its neighbors, because these frequencies depend on the atomic structure of the hydrogen-related defects.

To the best of our knowledge, the first infrared absorption study of hydrogen-related point defects in ZnO was made by Gärtner and E. Mollwo.^{7,8} They performed a detailed and thorough study of copper-doped ZnO annealed in a hydrogen atmosphere, and identified a set of LVM's originating from different copper-hydrogen defects.

Here, we report on the results of an infrared absorption study of nominally undoped ZnO treated with a hydrogen

plasma. Three new infrared absorption lines at 3611.3, 3349.6, and 3312.2 cm^{-1} have been detected. The 3611.3- cm^{-1} line is tentatively identified as the LVM of BC hydrogen, and the other two modes as LVM's of a zinc vacancy having two hydrogen atoms.

II. EXPERIMENTAL DETAILS

The ZnO crystals used in this work were hexagonal prisms with a diameter of about 2 mm and a length of ~ 20 mm. The nominally undoped n -type ZnO single crystals with resistivities of 10–100 Ω cm were grown from the vapor phase at the Institute for Applied Physics, University of Erlangen, Germany.^{9,10}

The samples were exposed for 1–19 h to a remote hydrogen and/or deuterium dc plasma in a parallel-plate system, with a plate voltage of 1000 V. The samples were mounted on a heater block held at a temperature of 150–380 $^\circ\text{C}$ and placed 10 cm downstream from the plasma with a bias voltage of about 300 V, which fixed the bias current to ~ 40 μA . The gas pressure was held at ~ 1 mbar.

In order to study the annealing behavior of the absorption lines, infrared absorbance spectra were recorded at 9 K after each step in a series of isochronal heat treatments (annealings) at temperatures in the range 400–700 $^\circ\text{C}$. The annealings were performed in a furnace purged with argon gas and the duration of each treatment was 30 min.

Infrared absorbance spectra were recorded at normal incidence with a BOMEM DA3.01 Fourier-transform spectrometer equipped with a global light source, a KBr beam splitter, and a liquid-nitrogen-cooled mercury cadmium telluride detector. To avoid mounting stress, the samples were free standing in the sample compartment of an exchange-gas cryostat, where the temperature was measured with a platinum resistor. The measurements were performed in the temperature range 9–120 K. Polarized light was produced by putting a wire-grid polarizer with KRS-5 substrate in front of the cryostat.

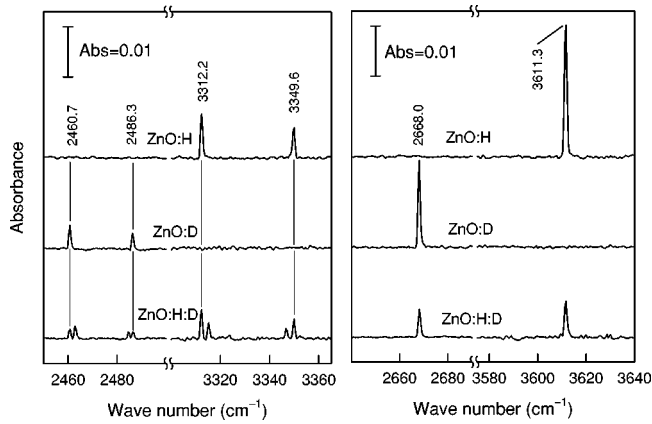


FIG. 1. Absorption spectra measured for ZnO samples at 10 K after H-, D-, and (H+D)-plasma treatments at 350 °C. $\mathbf{k} \perp c$. Unpolarized light.

III. RESULTS

A. Isotope shifts

Figure 1 shows typical infrared absorption spectra measured at 9 K for a ZnO sample after exposure to a hydrogen and/or deuterium plasma at 350 °C for 2 h. The spectra have been measured with the c axis of the crystal perpendicular to the beam, $\mathbf{k} \perp c$. Three new absorption lines at 3611.3, 3349.6, and 3312.2 cm^{-1} are seen in the hydrogen-treated sample (top spectra). The frequency range of 3400–3800 cm^{-1} is typical for oxygen-hydrogen stretch modes.^{7,11} When hydrogen is substituted by deuterium (midspectra), the lines shift downwards in frequency to 2668.0, 2486.3, and 2460.7 cm^{-1} , respectively. The frequency ratios of the hydrogen and deuterium-related lines are 1.35, which is close to the value expected for a harmonic oscillator consisting of a hydrogen atom bound to an oxygen atom, $\sqrt{m_r^D/m_r^H} = 1.37$, where m_r^H and m_r^D are the reduced masses of the $^{16}\text{O-H}$ and $^{16}\text{O-D}$ units, respectively. The LVM frequencies strongly suggest that the new lines are stretch LVM's of O-H species. When the sample is treated with hydrogen and deuterium plasma, four additional lines at 3346.6, 3315.2, 2484.6, and 2463.0 cm^{-1} (bottom spectra in Fig. 1) are observed. No extra lines are seen near the 3611.3- and 2668.0- cm^{-1} lines. This implies, that two different defects are responsible for the 3611.3-, 3349.6-, and 3312.2- cm^{-1} lines. The LVM at 3611.3 cm^{-1} belongs to a defect containing one hydrogen atom, whereas the LVM's at 3349.6 and 3312.2 cm^{-1} originate from a defect containing two *non-equivalent* hydrogen atoms. From now on, we call these defects H-I and H-II, respectively.

Figure 2 shows the results of isochronal annealing experiments on ZnO samples treated with a hydrogen plasma at 350 °C. Indeed, the LVM's of the H-II defect (the 3349.6- and 3312.2- cm^{-1} lines) retain the same relative intensity, regardless of the annealing temperature, which confirms the above suggestion that they belong to the same defect. It follows also from the figure that the H-I defect anneals out at 500 °C, whereas H-II is more stable and disappears from the spectra at 600 °C. Parallel to the annealing of H-I and H-II, another line at 3191.6 cm^{-1} grows in the spectra. It repre-

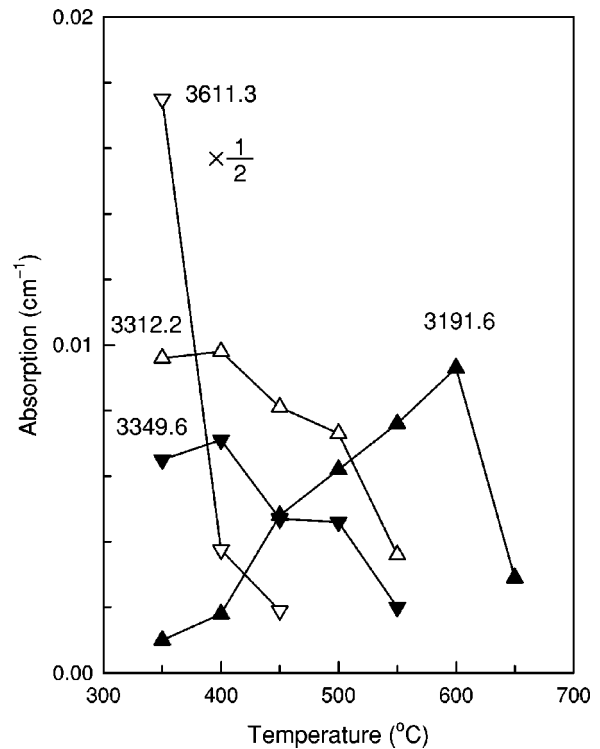


FIG. 2. The intensity (integrated absorbance) of the 3191.6- cm^{-1} (\blacktriangle), 3312.2- cm^{-1} (\triangle), 3349.6- cm^{-1} (\blacktriangledown), and 3611.3- cm^{-1} (\triangledown) lines measured at 10 K for a ZnO sample treated with hydrogen plasma at 350 °C and subsequently annealed.

sents a stretch LVM of the well-known Cu-H defect.^{7,8} It reaches its maximum intensity at 600 °C, when both H-I and H-II are already gone from the spectra.

B. Polarization dependences

The results of polarization dependent absorption measurements are presented in Fig. 3. It shows the normalized intensities of the LVM's belonging to the H-I and H-II defects as a function of the polarizer angle (θ) with respect to the c axis of the sample. It follows from the figure that the LVM of

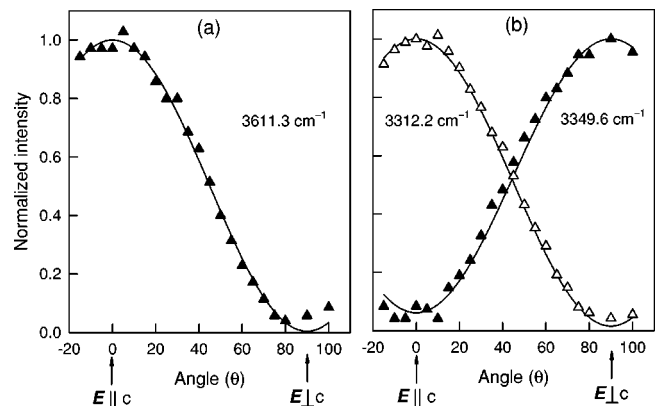


FIG. 3. Normalized LVM intensities of the H-I (a) and H-II (b) defects measured at 10 K as a function of the angle θ between polarizer and the c axis of the sample; $\mathbf{k} \perp c$. Solid lines—fit from Eq. (1).

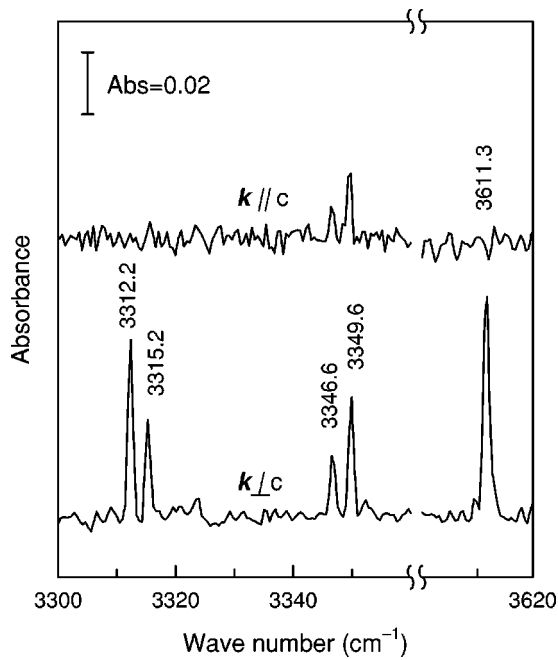


FIG. 4. Absorption spectra measured at 10 K for ZnO samples after (H+D) plasma treatment at 350 °C; (a) $k \perp c$, (b) $k \parallel c$. (Unpolarized light.)

H-I and the LVM of H-II at 3312.2 cm^{-1} are fully polarized along the c axis, whereas the LVM of H-II at 3349.6 cm^{-1} is fully polarized perpendicular to c . Thus, the transition dipole moments responsible for the 3611.3 - and 3312.2-cm^{-1} lines lie along the c axis, whereas the transition moment responsible for the 3349.6-cm^{-1} line is nearly perpendicular to c .

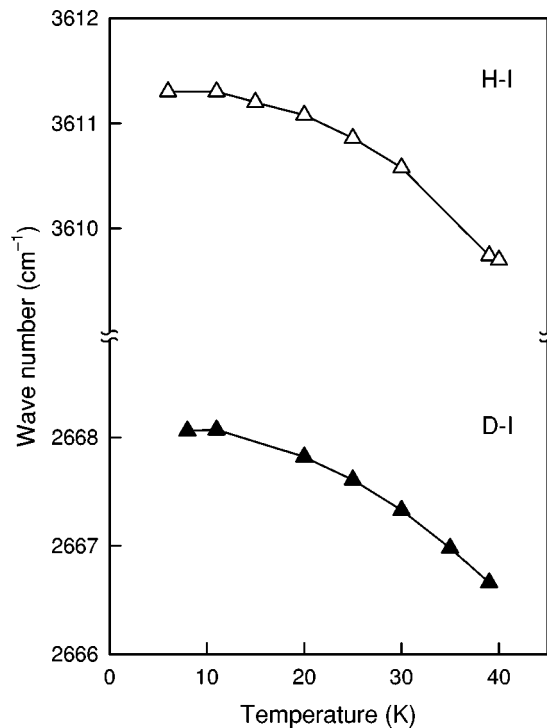


FIG. 5. Temperature dependences of the LVM frequencies of the H-I center measured after (H+D) plasma treatment at 380 °C.

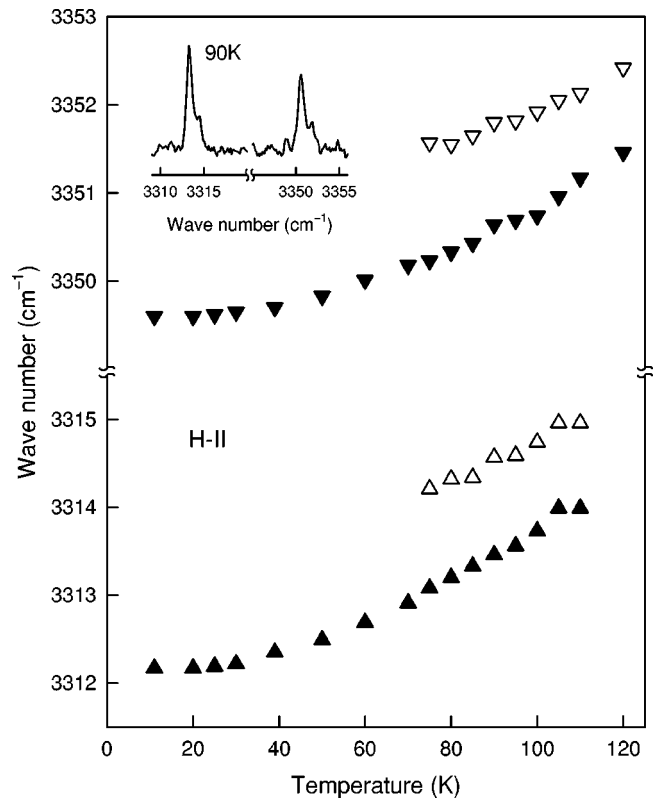


FIG. 6. Temperature dependence of the LVM frequencies of the H-II center measured after (H+D) plasma treatment at 380 °C. The inset shows a section of the absorption spectrum measured at 90 K.

This also can be seen in Fig. 4, which shows unpolarized absorption spectra measured with $k \parallel c$ and $k \perp c$ for ZnO samples treated with hydrogen and deuterium plasma at 350 °C. In case of $k \parallel c$, the LVM's with transition moments parallel to the c axis are not excited, whereas the LVM's related to the dipole moments perpendicular to the c axis (3347 and 3350 cm^{-1}) are still clearly seen in the spectrum.

C. Temperature data

Positions of the LVM's of the H-I and H-II defects as a function of temperature are shown in Figs. 5 and 6, respectively. According to Fig. 5, the LVM's of H-I shift downwards in frequency when the temperature rises. In contrast, the LVM's of the H-II defect shift upwards in frequency with the temperature (see Fig. 6). More interestingly, starting from about 70 K, another pair of LVM's shows up in the spectra, with frequencies $\sim 1 \text{ cm}^{-1}$ higher than the low-temperature LVM's. The same behavior is observed when hydrogen is substituted by deuterium, but the frequency shift between high and low LVM's is only $\sim 0.6 \text{ cm}^{-1}$, which is roughly a factor of $\sqrt{2}$ less than for the hydrogen-related LVM's. These frequency differences do not depend on the temperature but the line intensities of the high-frequency LVM's increase when the temperature rises. Simultaneously, all the lines become broader and, at temperatures above 110 K, the two sets of LVM's merge.

The relative intensities of the high-frequency mode (I_e) to the low-frequency one (I_g), $\Delta = I_e/I_g$, as a function of tem-

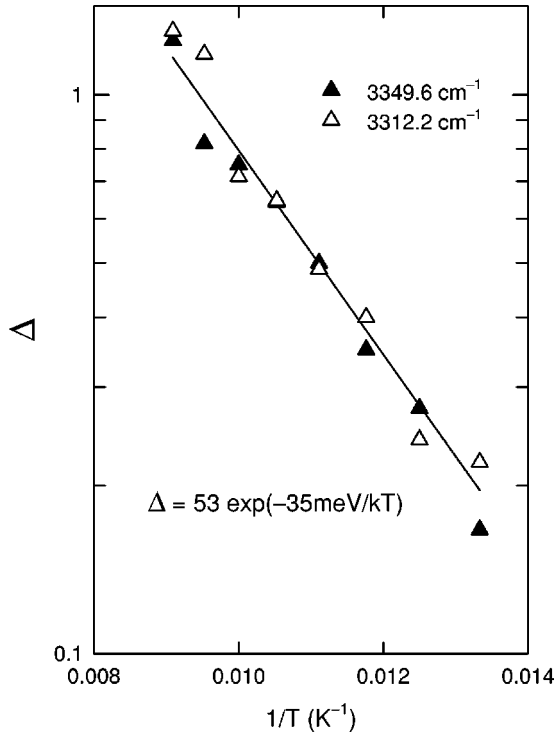


FIG. 7. Intensity ratio ($\Delta = I_e/I_g$) of the 3312.2- cm^{-1} (\triangle) and 3349.6- cm^{-1} (\blacktriangle) lines as a function of temperature, measured for a ZnO sample treated with (H+D) plasma at 380 °C. Solid line—fit by formula $\Delta = 53 \exp(-35 \text{ meV}/kT)$.

perature, are plotted in Fig. 7. The solid line is a least-squares fit by the function $\Delta = K \exp(-E_0/kT)$, where $K = 50 \pm 30$ and $E_0 = 35 \pm 5$ meV.

IV. CALCULATIONS

We have performed first-principles calculations based on density-functional theory within the local-density approximation and the pseudopotential-plane-wave method. Wurtzite supercells containing 96 atoms were used. Tests showed only minor differences between 32-atom and 96-atom supercells, ensuring that the results are converged as a function of supercell size. The effects of the Zn 3*d* states were included using the nonlinear core correction, with an energy cutoff of 40 Ry. Details and references can be found in Ref. 4.

In order to calculate vibrational frequencies we use the following approach.¹² For a given impurity or complex, we calculate the atomic configurations and total energies of stable and metastable configurations (global minimum and local minima in the potential-energy surface), including relaxation of the host atoms. The frequencies of the experimentally observed LVM's are strongly indicative of O-H bonds; indeed, Zn-H bonds would result in significantly lower frequencies. We have therefore focused on configurations that involve hydrogen bonded to oxygen atoms. The vibrational stretching modes for a given configuration are investigated by introducing small displacements of the H atom along the direction of the O-H bond in both positive and negative directions. The change of total energy as a function of distance results in a potential-energy curve, from which we can cal-

TABLE I. Vibrational properties for O-H bond-stretching modes in various configurations, calculated in 96-atom supercells (see text). Values for O-H on a nonpolar surface are included for comparison. $d_{\text{O-H}}$ is the O-H distance, in angstroms. ω^0 is the harmonic component of the vibrational frequency, $\Delta\omega$ is the anharmonic contribution, and ω is the total frequency ($\omega = \omega^0 + \Delta\omega$). All frequencies are in cm^{-1} . To facilitate comparison with experimental frequencies, we add 144 cm^{-1} (the difference between calculated and experimental values for O-H on the surface) to ω , resulting in the values ω^c listed in the last column.

Type	Configuration	$d_{\text{O-H}}$ (Å)	ω^0	$\Delta\omega$	ω	ω^c
O-H	surface	0.998	3624	-271	3353	3497
H ⁺	BC	0.990	3735	-235	3500	3644
H ⁺	AB _{O,}	1.006	3481	-273	3208	3352
V _{Zn} H ₂	O-H <i>c</i>	1.008	3420	-336	3084	3228
V _{Zn} H ₂	O-H _⊥ <i>c</i>	1.008	3415	-344	3072	3216

culate the vibrational frequency, using the reduced mass of the O-H unit. The potential-energy curves are highly nonparabolic, and we explicitly evaluate anharmonicity.¹²

An explicit comparison with a known experimental configuration was performed by calculating the stretch mode for an O-H bond on a nonpolar ZnO surface, resulting in a frequency of 3353 cm^{-1} . Experimental values of 3497 cm^{-1} and 3495 cm^{-1} were reported in Refs. 13 and 14, respectively. Our computational value thus underestimates the experimental number by about 144 cm^{-1} ; this deviation is due to a combination of numerical approximations, probably mainly due to the specific pseudopotentials chosen for the present study. Given the similarities in bonding configurations for all the O-H bonds investigated in the present study, this error is expected to be largely systematic, and we suggest adding 144 cm^{-1} to all our calculated values (see Table I). Even after this systematic correction, we still estimate the error bars on our calculated frequencies to be of the order of $\pm 100 \text{ cm}^{-1}$.

The configurations that have been investigated for the present study include isolated interstitial H⁺ in the BC and AB configurations, and hydrogen bound in a zinc vacancy. The energetics of interstitial H⁺ were described in Ref. 4, and the results for vibrational frequencies are given in Table I. The symbol _{||} denotes the configuration with the O-H bond parallel to the *c* axis; the other bond directions are denoted by the symbol _⊥. We note that the more sophisticated computational approach for obtaining vibrational frequencies in the present work results in more accurate values than the preliminary numbers for harmonic frequencies included in Ref. 4.

The Zn vacancy is a double acceptor and occurs in the 2- charge state (V_{Zn}^{2-}) in *n*-type ZnO. This immediately suggests that the vacancy can be neutralized by binding two hydrogen atoms. We find, indeed, that the binding energy per H, referenced to interstitial H⁺, is 1.80 eV. Both of the hydrogens form O-H bonds “inside” the vacancy; our calculations for configurations involving H in AB position (“outside” the vacancy) resulted in much higher energies. One of the hydrogen atoms forms an O-H bond oriented approxi-

mately along the c axis (our calculations actually produce an angle with the c axis of 10°). The other hydrogen forms an O-H bond at an angle of 98° with the c axis; i.e., it is tilted away from the nominal Zn-O bond direction in the perfect crystal by about 11° , towards a direction perpendicular to the c axis.

We have calculated the vibrational modes of this complex assuming they are totally decoupled, an assumption that is supported by the small magnitude of the experimental frequency shifts for one of the O-H bonds when the other H is substituted by D. The results are listed in Table I.

V. DISCUSSION

A. Bond angles

The intensity of the light absorbed by the electrical dipole vibrating in ZnO can be written as

$$I \propto \sum_{R_k \in C_{3v}} |\mathbf{e} \cdot (\mathbf{R}_k \mathbf{d})|^2, \quad (1)$$

where \mathbf{e} is the polarization vector of the light, \mathbf{d} is the transition dipole moment, and \mathbf{R}_k is the symmetry operator of the C_{3v} point group. For the stretch modes, the direction of the dipole moment should coincide with the bond direction, provided each bond vibrates independently. Thus, from the polarization dependences shown in Fig. 3 we may obtain an angle φ between the O-H bond of a defect and the c axis of the crystal if the assumption of independent vibrations is valid.

H-I. The defect contains only one O-H bond, therefore the assumption that its direction coincides with the induced dipole moment is fulfilled automatically. The best fit to the experimental data, shown in Fig. 3(a) by the solid line, is achieved when the O-H bond is aligned with the c axis, i.e., $\varphi=0$. We note that within 10° all fitting curves are very close to the shown one. Thus, the O-H bond comprising the H-I defect is aligned with the c axis with a maximum deviation from the perfect [0001] direction of 10° .

H-II. The defect contains two O-H species and according to the isotope substitution data (see bottom spectrum in Fig. 1), the coupling between the two LVM's of the H-II defect is rather weak, i.e., substitution of one hydrogen atom comprising the defect with deuterium does not change considerably the local mode frequency of the other O-H bond. Thus, the O-H bonds of H-II vibrate independently, and from Eq. (1) we get directly the bond angles. The best fit to the data, shown in Fig. 3(b), is accomplished if we assume that the O-H bond responsible for the 3312.2-cm^{-1} line is aligned with the c axis with a maximum deviation from the perfect [0001] direction of 10° . The other O-H bond of the defect responsible for the 3349.6-cm^{-1} line is nearly perpendicular to the c axis, $\varphi=100\pm 5^\circ$, i.e., it is tilted from the perfect Zn-O bond "perpendicular" to the c axis by $\sim 10^\circ$.

From Eq. (1) and known angles φ , we may also estimate relative intensities of the 3349.6- and 3312.2-cm^{-1} lines if we assume that the effective charges of both O-H bonds are

equal. With this assumption, we obtain that $I_{3312}/I_{3350} = 1.46$, which is rather close to the experimental value of 1.6 ± 0.2 (see Fig. 2).

B. Tentative models

H-I. The experimental observations indicate that this defect has one hydrogen atom primarily bound to an oxygen atom with the O-H bond aligned close to the c axis. H-I is observed in all our nominally undoped ZnO samples. We propose that interstitial hydrogen at the BC_{\parallel} site is the most likely candidate for this center. Indeed, the first-principles calculations⁴ indicate that in this configuration hydrogen is strongly bound to an oxygen atom, with the neighboring Zn atom relaxing outward by almost 40% of the bond length. The results of Ref. 4 showed that the BC_{\parallel} , BC_{\perp} , AB_{\parallel} and AB_{\perp} configurations all have very similar formation energies, although calculations with increased convergence and additional relaxation performed as part of the present work indicate that BC_{\parallel} may be lower than the others by about 0.1 eV. The experimental results conclusively indicate a configuration oriented parallel to c , but experiment alone cannot distinguish between BC_{\parallel} and AB_{\parallel} . Both the calculated formation energies⁴ and the calculated vibrational frequencies (Table I) strongly favor BC_{\parallel} ; indeed, the calculated LVM for AB_{\parallel} is about 300 cm^{-1} lower than the LVM at BC_{\parallel} . All these findings point to interstitial hydrogen at BC_{\parallel} ($H_{BC_{\parallel}}^+$) as the most likely candidate for the H-I defect.

We cannot exclude that this interstitial hydrogen might be bound to an impurity. Indeed, the fact that the H-I signal is stable up to about 350°C in the annealing experiments (see Sec. III C) may point to a configuration that is more strongly bound than isolated interstitial hydrogen, which has a diffusion barrier of about 0.9 eV.¹⁵ The samples used in our study are known to contain impurities, but quantitative information is not available. Interstitial hydrogen bound to an isoelectronic or acceptor impurity could account for the H-I line, provided the hydrogen would still be in the BC_{\parallel} configuration.

One impurity that is known with certainty to be present in the samples is Cu. However, the Cu-H complex has been investigated in detail in previous experimental work^{7,8,17} and was found to have an LVM at 3191.6 cm^{-1} . In our current experimental work we indeed see a line with that frequency appearing upon annealing (see Fig. 2). It can be assumed that the Cu-H complex involves a H atom strongly bound to an oxygen neighbor of the Cu_{Zn} impurity. Explicit calculations for Cu-containing centers are beyond the scope of our present study, but we suggest that the H atom in Cu-H is located in an AB position, rather than a BC site. This would explain the significantly lower frequency observed for this center (see Table I). The reason for hydrogen favoring the AB position in the case of Cu could be related to the larger ionic radius of the Cu ion when it becomes negatively charged in the complex due to electron transfer from H to Cu.

We noted that the interstitial hydrogen responsible for H-I may be complexed with an impurity. Further studies in combination with other experimental techniques such as EPR,

electron-nuclear double resonance (ENDOR), etc., are called for. While we cannot identify the impurity at this time, we can exclude the possibility that hydrogen would be complexed with a native point defect. Since the complex should include strong O-H bonds, the possible candidates are V_{Zn} , oxygen interstitial (O_i) or oxygen antisites (O_{Zn}). We will argue below that V_{Zn} is actually associated with H-II. As to the oxygen interstitial and antisite, both of these defects have been found to be very high in energy,¹⁶ and thus very unlikely to be present in our samples.

It is known that the conductivity of ZnO crystals exposed to hydrogen increases.¹⁸ With our samples we have found that the resistivity is reduced from 50 to 5 Ω cm after hydrogen plasma treatment. This finding is definitely consistent with hydrogen being introduced as an interstitial and acting as a shallow donor. However, the resistivity data alone cannot help to distinguish between hydrogen being present as an isolated donor (H_{BC}^+) or passivating an acceptor impurity or native defect, since both scenarios increase the n -type conductivity of ZnO.

H-II. The defect has two nonequivalent hydrogen atoms primarily bound to oxygen atoms. It is observed in all our nominally undoped ZnO samples. One of the two O-H bonds comprising H-II is close to the c axis, whereas the other one is nearly perpendicular to c . Two interstitial hydrogen atoms, both acting as shallow donors, are unlikely to spontaneously come together, pointing strongly towards involvement of another defect. We have argued that V_{Zn} is the most likely candidate. Indeed, the Zn-H bond is much less stable as compared to the O-H bond, and the Zn-H stretch LVM frequencies should be in the range 1500–1700 cm^{-1} , which is too far from what we see in our spectra.¹¹ Thus, among the native defects, only V_{Zn} , O_i or O_{Zn} having two hydrogen atoms may explain our data. Interstitial oxygen and oxygen antisites are ruled out by the weak coupling between the two LVM's of H-II and by their high formation energies.¹⁶ Therefore, we propose that a zinc vacancy having two hydrogen atoms, $V_{\text{Zn}}\text{H}_2$, is the most probable model for H-II. This proposal is convincingly supported by our first-principles calculations as reported in Sec. IV. The calculated angles between the O-H bonds and the c axis are 10° and 98° , in good agreement with the experimental numbers (see Sec. V A). The calculated vibrational frequencies for $V_{\text{Zn}}\text{H}_2$ (Table I) are also in reasonable agreement with the experimental LVM's. And finally, the calculated binding energy of hydrogen in the Zn vacancy (1.8 eV per H, see Sec. IV) is consistent with the anneal temperature of the H-II LVM's (see Fig. 2).

This assignment is also supported by the results of cathodoluminescence studies of ZnO after hydrogen plasma treatment. Sekiguchi *et al.* have shown that such a treatment made at 400 $^\circ\text{C}$ fully suppresses the so-called “green” luminescence band centered around 2.2 eV.¹⁹ We have observed the same behavior by means of photoluminescence on our ZnO samples. On the other hand, based on first-principles pseudopotential calculations, Kohan *et al.* suggested that V_{Zn} is involved in the green luminescence in ZnO.¹⁶ Passivation of V_{Zn} with two hydrogen atoms thus leads to a reduction of the green luminescence, and appearance of the H-II LVM's.

As mentioned above, the resistivity of our ZnO samples is reduced from 50 to 5 Ω cm after hydrogen plasma treatment, which is also in favor of the the $V_{\text{Zn}}\text{H}_2$ model. Indeed, passivation of V_{Zn} acting as an acceptor in ZnO should increase the n -type conductivity of the samples.

It follows from the temperature data (see Fig. 6) that H-II has an excited state with an activation energy of 35 ± 5 meV. The high preexponential factor ($K=50 \pm 30$) as well as the independence of the excitation energy on the hydrogen isotope exclude the possibility that a low-frequency wag mode is involved in the excited states of the defect. However, coupling with another vibrational mode might lead to the observed behavior. In addition, we see two other possible models that may give rise to the excited states. The first possibility is the transition to another charge state. The activation energy of this transition fits rather well to the known ionization energies of shallow donors in ZnO.^{6,20–23} However, it is very difficult to envision that $V_{\text{Zn}}\text{H}_2$ may have a shallow donor state, or a deep state in which carriers released from shallow donors could be trapped.

Another possible explanation of the excited state of H-II comes from the polarization data (Sec. V A) indicating that the O-H bonds of H-II are not perfectly aligned with the regular Zn-O bonds of the crystal. This implies that apart from the global minimum, additional minima may exist, which could result in somewhat higher LVM's than those of the ground state. This situation, for example, has been observed for the VH defects in silicon.²⁴ The point group of the defect is C_{1h} , i.e., the Si-H bond is tilted from the perfect [111] direction. When the temperature rises, hydrogen jumps between different equivalent minima. The activation energy of the jump process has been found to be 60 ± 10 meV, which is comparable and somewhat higher than what we observe for H-II. The different local minima may involve displacements of the hydrogen and/or oxygen atoms, but the small magnitude (35 meV) of the energy difference between the ground-state and excited-state configurations and the lack of a significant barrier between them would make it very difficult to resolve these distinct configurations in first-principles calculations.

Finally, we would like to comment on the temperature dependences of the LVM frequencies of H-II. Normally, the LVM frequency of a defect increases with decreasing temperature resulting from strengthened bonds arising from the lattice contraction. In contrast, the LVM frequencies of H-II shift downwards with temperature (see Fig. 6). The same behavior has been observed for the oxygen dimer O_{2i} (Ref. 25) and for the hydrogen bend mode of the dicarbon-dihydrogen defect in Si.^{26,27} All these defects, such as H-II, have a common property, namely, one or more of the defect bonds is a nonaxial one. This might provide a possible explanation of the anomalous temperature behavior of the LVM frequency. A downward shift in the frequency with temperature is caused by the buckling of the defect atom from the regular bond direction.²⁸

VI. SUMMARY

Vibrational spectroscopy on ZnO samples hydrogenated using a H or a D plasma has produced three new infrared

(IR) absorption lines at 3611.3, 3349.6, and 3312.2 cm^{-1} . The first, at 3611.3 cm^{-1} , has been assigned to a defect labeled H-I, which contains a single H atom. Based on polarization studies and first-principles calculations we propose that H-I corresponds to an interstitial H atom at a BC_{\parallel} site, although the possibility that this H atom is associated with an impurity cannot be excluded. The lines at 3349.6 and 3312.2 cm^{-1} are associated with a defect labeled H-II that contains two hydrogen atoms, one in an O-H bond roughly aligned with the c axis, and the other in an O-H that forms an angle of 100° with the c axis. First-principles calculations for a hydrogenated Zn vacancy ($V_{\text{Zn}}\text{H}_2$) produce results

in good agreement with the experimental observations for H-II.

ACKNOWLEDGMENTS

We thank N. A. Yarykin (IMT RAS, Chernogolovka) for the help with electrical measurements, J. R. Botha (University of Port Elisabeth) for the help with photoluminescence measurements, B. Bech Nielsen (University of Aarhus) for helpful discussions, and S. Limpijumngong for help with the calculations. E.V.L. acknowledges the Russian Foundation for Basic Research (Grant No. 02-02-16030). C.V.d.W. acknowledges the Air Force Office of Scientific Research, Award No., F49620-02-1-1163.

*Also at Institute of Radioengineering and Electronics, Mokhovaya 11, 101999 Moscow, Russia. Electronic address: edward.lavrov@physik.phy.tu-dresden.de

¹D. C. Look *et al.*, Solid State Commun. **105**, 399 (1998).

²M. Joseph, H. Tabata, and T. Kawai, Jpn. J. Appl. Phys., Part 2 **38**, L1205 (1999).

³D. C. Look, J. W. Hemsky, and J. R. Sizelove, Phys. Rev. Lett. **82**, 2552 (1999), and references therein.

⁴C. G. Van de Walle, Phys. Rev. Lett. **85**, 1012 (2000).

⁵S. F. J. Cox *et al.*, Phys. Rev. Lett. **86**, 2601 (2001).

⁶Detlev M. Hofmann *et al.*, Phys. Rev. Lett. **88**, 045504 (2002).

⁷F. G. Gärtner and E. Mollwo, Phys. Status Solidi B **89**, 381 (1978).

⁸F. G. Gärtner and E. Mollwo, Phys. Status Solidi B **90**, 33 (1978).

⁹G. Müller and R. Helbig, J. Phys. Chem. Solids **32**, 1971 (1971).

¹⁰R. Helbig, J. Cryst. Growth **15**, 25 (1972).

¹¹*CRC Handbook of Chemistry and Physics*, 82nd ed., edited by David R. Lide (CRC Press, LLC, 2001), pp. 9–77.

¹²C. G. Van de Walle, Phys. Rev. Lett. **80**, 2177 (1998).

¹³R. P. Eischens, W. A. Pliskin, and M. J. D. Low, J. Catal. **1**, 180 (1962).

¹⁴G. Ghiotti, A. Chiorino, and F. Boccuzzi, Surf. Sci. **287/288**, 228 (1993).

¹⁵D. G. Thomas and J. J. Lander, J. Chem. Phys. **25**, 1136 (1956).

¹⁶D. Zwingel, Phys. Status Solidi B **67**, 507 (1975).

¹⁷A. F. Kohan, G. Ceder, D. Morgan, and C. G. Van de Walle, Phys. Rev. B **61**, 15 019 (2000).

¹⁸E. Mollwo, Z. Phys. **138**, 478 (1954).

¹⁹T. Sekiguchi, N. Ohashi, and Y. Terada, J. Appl. Phys. **36**, L289 (1997).

²⁰J. Schneider and A. Räuber, Z. Naturforsch. A **16A**, 712 (1961).

²¹P. Wagner and R. Helbig, J. Phys. Chem. Solids **35**, 327 (1974).

²²M. Schulz, Phys. Status Solidi A **27**, K5 (1975).

²³D. Block, A. Herve, and R. T. Cox, Phys. Rev. B **25**, 6049 (1982).

²⁴B. Bech Nielsen, P. Johannesen, P. Stallinga, and K. Bonde Nielsen, Phys. Rev. Lett. **79**, 1507 (1997).

²⁵S. Öberg, C. P. Ewels, R. Jones, T. Hallberg, J. L. Lindström, L. Murin, and P. R. Briddon, Phys. Rev. Lett. **81**, 2930 (1998).

²⁶E. V. Lavrov, L. Hoffmann, B. Bech Nielsen, B. Hourahine, R. Jones, S. Öberg, and P. R. Briddon, Phys. Rev. B **62**, 12 859 (2000).

²⁷E. V. Lavrov, L. Hoffmann, and B. Bech Nielsen (unpublished).

²⁸J. Coutinho, R. Jones, P. R. Briddon, and S. Öberg, Phys. Rev. B **62**, 10 824 (2000).